Review

A Collaborative Robust Scheduling Model for Flexibility Resources of Source, Grid, Load, and Storage in the New Power System

Yanyu Wang[1], Yuxin Tai[1], Ting Wang[1], Tao Ling[2]*, Guangjun Liu[1], Dong Dou[1], Wei Fan[2, 3]

[1]Inner Mongolia Electric Power Economics and Technology Research Institute, Hohhot, Inner Mongolia, China
[2]School of Economics and Management, Beihang University, Beijing, China
[3]Beijing Energy Development Research Center, Beijing, China

Abstract

The power generation of renewable energy sources is directly related to meteorological conditions like wind speed and sunlight. Integrating large-scale unstable power sources into the power system generates a need for adjustment and introduces operational risks. To improve the system's adjustment performance and address the impact of uncertainties, this paper analyzes the operational characteristics and adjustment differences of various flexible resources and proposes a collaborative robust scheduling model for multi-flexible resources of source, grid, load, and storage, considering multiple uncertainties. The model aims to minimize system operation costs, including technical modifications, fuel consumption, start-up and shutdown, and energy curtailment, while satisfying constraints such as real-time supply-demand balance, system adjustment margin, and unit operation. An improved robust optimization theory is introduced to handle the uncertainties in renewable energy, transforming the model into an easier-to-solve problem. Finally, the case study results show that various flexible resources of source-grid-load-storage have different adjustment performances, and all types of resources are indispensable for a power system with a high proportion of renewable energy. Applying the proposed collaborative robust scheduling model can achieve a balanced decision-making process between risk and economy, ensuring complementary advantages and optimal allocation of various source-grid-load-storage resources.

Keywords: new power system, source-grid-load-storage, flexible resources, light robust optimization, scheduling model

*e-mail: 18205917084@163.com
Tel.: +86-182-0591-7084.

Introduction

Climate change has become a challenge faced by all of humanity, and achieving carbon neutrality has become a global consensus and strategic choice in addressing and mitigating climate change. With their clean and low-carbon advantages, renewable energy sources such as wind power and photovoltaics are experiencing unprecedented development opportunities. By the end of 2023, the installed capacity of wind power and photovoltaics in China accounted for 36% of the total [1]. Due to the significant variability and intermittency in the spatiotemporal distribution of wind power and photovoltaic generation, their uncertainty is much greater than the load's, and their temporal variation patterns are not synchronized with load curves [2]. Studies have shown that the high proportion of wind power and photovoltaic integration brings new challenges to the flexibility requirements and secure and stable operation of the power system [3]. Therefore, the reasonable allocation and efficient utilization of flexible resources of source, grid, load, and storage have become core factors in maintaining real-time power supply-demand balance and are key to the high-quality development of the new power system.

Recently, the flexibility of the power system has drawn significant attention from scholars, as it encompasses a wide range of meanings. Whether considering the power fluctuations of renewable energy on the supply side or the randomness of electric vehicle charging on the demand side, both impose higher requirements on the flexibility of the power system [4]. The International Energy Agency (IEA) [5] proposed the concept of flexibility, referring to the ability to respond to foreseeable and unforeseeable fluctuations on both the supply and demand sides while considering economic efficiency. Huang et al. [6] define power system flexibility as the ability to respond to changes in net load within a predetermined time frame. In this paper, flexibility is viewed as a broader concept, referring to the power system's adaptability to various changes, encompassing aspects such as stability, reliability, and adequacy. This includes not only the ability to respond to different time scales (e.g., hours, minutes) but also the capacity to handle various types of risks (e.g., power fluctuations, outages). Flexibility is key to the operation of the power system and requires ensuring sufficient power supply security at all times.

The enhancement of power system flexibility relies on various flexible resources, which are widely distributed across different power system sectors. Scholars have conducted in-depth studies on various types of flexible resources. Wang et al. [7] compared the performance of different coal-fired power units from a flexibility perspective and analyzed the impact of flexibility retrofitting technologies on the adaptability of renewable energy. Jin et al. [8] explored the regulatory role of cascade hydropower in the power system and found that wind and photovoltaic power generation can

reduce the adjustment efficiency of hydropower. Qin et al. [9] provided a comprehensive comparison and review of various long-distance transmission technologies, highlighting that long-distance, high-capacity transmission lines can mitigate the issue of the inverse distribution between renewable energy production and consumption. Cui et al. [10] considered the electricity consumption preferences of different types of users and developed a demand response model for multi-type user loads, revealing the importance of load control for the secure operation of the power system. Chen et al. [11] constructed a multi-temporal storage capacity expansion model that considers both the characteristics of renewable energy generation and the load demand at the receiving end, analyzing the demand scale for various storage technologies with different durations. As the proportion of variable renewable energy increases, the adjustment potential of resources of source, grid, load, and storage sectors cannot be overlooked. Existing research suggests that the adjustment methods and performance of flexible resources vary. It is necessary to guide them to actively participate in system regulation, such as auxiliary service mechanisms.

The collaborative operation of a power system's source, grid, load, and storage refers to optimizing and integrating resources such as power generation, transmission, distribution, and storage to reduce energy usage costs and improve energy efficiency [12]. Hao et al. [13] pointed out that the spatial and temporal symmetry between source and load is of significant importance for resource allocation in the power system. In their work, they proposed the concept of distribution-side source-load symmetry and analyzed its impact on the optimal scheduling of distribution networks. However, they did not consider the influence of energy storage on source-load symmetry. Yang et al. [14] proposed an optimized electrothermal system model for collaborative hydrogen production by integrating generation, load, and storage, considering refined flexible load response. However, they did not explore the potential of the transmission network to accommodate renewable energy. Xiang et al. [15] developed an expansion planning model for distribution systems based on the coordination of source, grid, load, and storage, enhancing the adaptability of distribution networks to renewable energy. The aforementioned studies primarily focused on traditional power system dispatching, focusing on the balance of power supply and demand, without examining the adjustment potential of collaborative operation from a flexibility perspective. However, this is a critical issue in building a power system with a high proportion of renewable energy, which is the focus of this paper.

The above research indicates that the economic scheduling model can incorporate flexible resources of source, grid, load, and storage into a unified framework, aiming for cost minimization to optimize resource allocation [16]. Since a secure electricity supply is a fundamental guarantee for social and economic

development, the operational risks of power systems are also worth attention, particularly during the current rapid development of renewable energy [17, 18]. With the increasing penetration of wind and photovoltaic power, as well as the growing concerns about climate change, the uncertainty associated with hydropower must not be overlooked. Some researchers have employed deep learning and machine learning methods to improve the accuracy of renewable energy and load forecasting [19]. Additionally, other scholars have focused on enhancing the power system's optimization and scheduling methods to improve their reliability. Robust optimization, a pre-analysis method in uncertain optimization, evolved from robust control theory and has been widely applied in uncertain power system dispatch [20]. Attarha et al. [21] constructed a polyhedral uncertainty set to address the uncertainties of wind power and system load, proposing a robust optimal power flow model for the power system. As the application of the model deepened, scholars identified drawbacks in the robust optimization model, particularly its conservative nature, as constraints must be strictly adhered to, leading to decisions that may not align with real-world scenarios [22]. Consequently, the robust optimization model has undergone improvements, such as the development of the distributionally robust optimization model [23]. Esfahani et al. [24] employed a data-driven distributionally robust optimization theory to characterize the uncertainty of production and consumption behavior, yielding results that mitigated conservatism. This paper adopts another approach to relax and improve the robust optimization theory, offering advantages such as faster solution speed and reduced conservatism.

In summary, existing research has already focused on the flexibility of power systems with a high proportion of renewable energy and has produced abundant results in the field of secure and economic scheduling. However, these studies did not focus on the differences in resource regulation performance between different links of the source network load storage, only on the results of whether the power supply and demand are balanced, and did not analyze the complementarity of these resources from the perspective of flexibility. Additionally, there is still considerable room for improvement in robust optimization models for addressing uncertainties, requiring more practical and efficient optimization strategies. Therefore, this paper proposes a collaborative robust scheduling model for flexible resources of source, grid, load, and storage, with the main contributions and innovations as follows:

(1) In terms of perspective, this paper explores the flexibility of a power system with a high proportion of renewable energy, delving into the new challenges and adjustment demands that power systems face in the context of large-scale renewable energy integration. Focusing on the volatility and uncertainty of renewable energy sources such as wind power and photovoltaics, the paper proposes collaborative scheduling strategies for flexible resources.

(2) In terms of research content, a comprehensive optimization and scheduling framework for flexible resources of source, grid, load, and storage is designed. The study emphasizes these resources' adjustment potential and complementary advantages when coordinating. Additionally, scenarios are set up to compare the differences in power system flexibility under various combinations of source, grid, load, and storage resources.

(3) In terms of research methodology, the traditional robust optimization theory is improved by constructing a light robust optimization model. The model balances system operation costs and risks by introducing relaxation variables and polyhedral uncertainty sets. The improved model reduces conservatism and enhances the adaptability of the power system.

The remainder of the paper is organized as follows: Section 2 analyzes the collaborative operation mechanism of flexible resources of source, grid, load, and storage. Section 3 constructs the collaborative scheduling model for flexible resources. Section 4 improves the robust optimization method. Section 5 presents a case study analysis. Section 6 provides conclusions and an outlook.

Material and Methods

Collaborative Mechanisms for Flexible Resources

Flexible Resources Classification and Characteristics

In the new power system with a high proportion of wind power (WP) and photovoltaic power (PV) integration, sufficient flexible resources are required to adjust and ensure a real-time dynamic balance of power supply and demand. Flexible resources can be classified into four categories based on different functional roles: source, grid, load, and storage. Table 1 shows the main classification and characteristics of flexible resources considered in this paper.

Operation Model for Flexible Resources

(1) Coal-fired power
Coal-fired power produces electricity by burning coal, and coal consumption can be approximately considered as a linear function of power output. Coal-fired power units have large unit capacities and stable operation. However, without flexibility transformation, they maintain a high minimum output, have slow ramp rates, and require long start-up and shutdown times. The operational model for coal-fired power is as follows:

$$F_{CP,i,t}^{coal} = \rho^{coal} b_{CP,i} P_{CP,i,t} \tag{1}$$

$$F_{CP,i,t}^{UD} = u_{i,t}^{up} F_{CP,i}^{up} + u_{i,t}^{down} F_{CP,i}^{down} \tag{2}$$

Table 1. Flexibility resources classification and characteristics.

Classification	Resources	Operation characteristics	Regulation range	Regulation speed
Source	Coal-fired power, (CP)	Fast adjustment, limited range, slow start and stop	50%~100%	1%-2%
	Flexibility transformation CP, (FT-CP)	Fast adjustment, expanded downward range, fast start and stop	30%~100%	3%-6%
	Regulated hydropower, (HP)	Fast adjustment, seasonal differences	0%~100%	20%
Grid	Transmission line, (TL)	Dependent on the receiving end, limited adjustment	-100%~100%	<1%
Load	Flexible load, (FL)	Incentive-driven, fast response	3%~5%	100%
Storage	Energy storage, (ES)	Fast adjustment, short duration, small scale	-100%~100%	100%

$$u_{i,t}\alpha_{CP,i}^{\min}C_{CP,i} \le P_{CP,i,t} \le u_{i,t}\alpha_{CP,i}^{\max}C_{CP,i} \tag{3}$$

$$-\beta_{CP,i}^{down}C_{CP,i} \le P_{CP,i,t} - P_{CP,i,t-1} \le \beta_{CP,i}^{up}C_{CP,i} \tag{4}$$

$$u_{i,t} - u_{i,t-1} - u_{i,t}^{up} \le 0 \tag{5}$$

$$u_{i,t-1} - u_{i,t} - u_{i,t}^{down} \le 0 \tag{6}$$

$$u_{i,t} - u_{i,t-1} - u_{i,k} \le 0, \forall k \in [t, T_i^{on} + t - 1] \tag{7}$$

$$u_{i,t-1} - u_{i,t} + u_{i,k} \le 1, \forall k \in [t, T_i^{off} + t - 1] \tag{8}$$

where the subscript i denotes the index of coal-fired power units, and the subscript t denotes the time index. $F_{CP,i,t}^{coal}$ is the fuel cost of coal-fired power, ρ^{coal} is the coal price, and $b_{CP,i}$ is the coal consumption rate. $P_{CP,i,t}$ denotes the power output of the coal-fired unit. $F_{CP,i,t}^{UD}$ denotes the start-up and shutdown costs, with $F_{CP,i}^{up}$ and $F_{CP,i}^{down}$ being the start-up and shutdown costs for a single operation, respectively. $u_{i,t}^{up}$ and $u_{i,t}^{up}$ are 0-1 binary variables indicating start-up and shutdown actions of the coal-fired unit, respectively. $u_{i,t}$ denotes the operational status of the coal-fired unit, with a value of 0 or 1. $C_{CP,i}$ is the rated capacity of the coal-fired unit. $\alpha_{CP,i}^{\min}$ and $\alpha_{CP,i}^{\max}$ denote the minimum and maximum output percentages, respectively. $\beta_{CP,i}^{down}$ and $\beta_{CP,i}^{up}$ are the ramp-up and ramp-down limits, respectively. T_i^{on} and T_i^{off} are the coal-fired unit's minimum on-time and minimum off-time, respectively.

(2) Flexibility transformation CP

The flexible transformation of coal-fired power offers significant economic advantages, making it a primary source of flexibility. After transformation, the minimum output is reduced, the ramp rate is increased, and the start-up time is shortened. The operational model of coal-fired power plants after transformation is similar to the previous one. The differences lie in the addition of transformation costs, an increase in coal consumption rate under low-load conditions, and optimized unit

adjustment parameters [25]. After the coal-fired power flexibility transformation, the operation model still needs to meet the requirements of formulas (1), (2), (5), and (6), but the parameters in formulas (3), (4), (7), and (8) have changed.

$$F_{FTCP,j,t}^{FT} = \rho^{FT}P_{FTCP,j,t} \tag{9}$$

$$u_{j,t}\hat{\alpha}_{FTCP,j}^{\min}C_{FTCP,j} \le P_{FTCP,j,t} \le u_{j,t}\alpha_{FTCP,j}^{\max}C_{FTCP,j} \tag{10}$$

$$-\hat{\beta}_{FTCP,j}^{down}C_{FTCP,j} \le P_{FTCP,j,t} - P_{FTCP,j,t-1} \le \beta_{FTCP,j}^{up}C_{FTCP,j} \tag{11}$$

$$u_{j,t} - u_{j,t-1} - u_{j,l} \le 0, \forall l \in [t, \hat{T}_j^{on} + t - 1] \tag{12}$$

$$u_{j,t-1} - u_{j,t} + u_{j,l} \le 1, \forall l \in [t, \hat{T}_j^{off} + t - 1] \tag{13}$$

where the subscript j represents the index of coal-fired power units after flexibility transformation, $F_{FTCP,j,t}^{FT}$ denotes the cost of the flexibility transformation for coal-fired power plants. ρ^{FT} denotes the transformation investment cost allocated per unit of power. The parameters with an $\wedge$ above the symbols indicate the optimized parameters of coal-fired power plants after the flexibility transformation.

(3) Regulated hydropower

Hydropower has strong adjustment capabilities, with very fast ramp-up and start-up rates, so ramping and start-up constraints can be ignored. The generation capacity of hydropower is related to water inflow and exhibits seasonal variations. Therefore, water allocations for regulated hydropower need to be scheduled over a long-term annual timescale. The operational model for hydropower is as follows:

$$F_{HP,t} = \rho_{HP}P_{HP,t} \tag{14}$$

$$\alpha_{HP}^{\min}C_{HP} \le P_{HP,t} \le \alpha_{HP}^{\max}C_{HP} \tag{15}$$

$$\sum_{t=1}^{T} P_{HP,t} \leq E_{HP} \tag{16}$$

where $F_{HP,t}$ denotes the cost of hydropower, ρ_{HP} denotes the unit generation cost of hydropower. $P_{HP,t}$ is the power output of the hydropower unit. C_{HP} is the rated capacity of the hydropower unit. $\alpha_{HP,i}^{min}$ and $\alpha_{HP,i}^{max}$ are the minimum and maximum output percentages, respectively. $E_{HP,t}$ is the amount of electricity allocated to a typical day based on the annual generation plan.

(4) Transmission line

The power of the transmission line is primarily determined by the receiving end. When local generation at the receiving end cannot meet its load, the sending end optimizes the cross-regional allocation of electricity through the transmission network. Transmission lines can enhance the security and reliability of the receiving end and increase the capacity for renewable energy accommodation at the sending end. The flexible adjustment model for transmission lines is as follows:

$$F_{TL,t} = \rho_{TL} P_{TL,t} \tag{17}$$

$$\lambda_{TL}^{min} C_{TL} \leq P_{TL,t} \leq \lambda_{TL}^{max} C_{TL} \tag{18}$$

where $F_{TL,t}$ denotes the transmission cost. ρ_{TL} denotes the unit transmission cost. $P_{TL,t}$ denotes the power of the transmission line. C_{TL} denotes the rated capacity of the transmission line. λ_{TL}^{min} and λ_{TL}^{max} are the minimum and maximum output percentages, respectively.

(5) Flexible load

Flexible load participation in demand response can be categorized into Transferable Flexible Load (TFL) and Interruptible Flexible Load (IFL). Transferable flexible loads, such as electric vehicle charging, can change usage times. Interruptible flexible loads, such as industrial manufacturers, can reduce consumption during peak load periods [26]. The flexible adjustment model for flexible load is as follows:

$$F_{FL,t} = \rho_{TFL}^{in} L_{TFL,t}^{in} + \rho_{IFL} L_{IFL,t} \tag{19}$$

$$\sum_{t=1}^{T} L_{TFL,t}^{in} = \sum_{t=1}^{T} L_{TFL,t}^{out} \tag{20}$$

$$0 \leq L_{TFL,t}^{in} \leq \delta_{TFL}^{max} L_t^0 \tag{21}$$

$$0 \leq L_{TFL,t}^{out} \leq \delta_{TFL}^{max} L_t^0 \tag{22}$$

$$0 \leq L_{IFL,t} \leq \delta_{IFL}^{max} L_t^0 \tag{23}$$

where $F_{FL,t}$ denotes the demand response cost, ρ_{TFL}^{in} and ρ_{IFL} denote the unit costs for load transfer and interruption, respectively. $L_{TFL,t}^{in}$ and $L_{TFL,t}^{out}$ denote the amounts of transferable load transferred in and out, respectively. δ_{TFL}^{max} denotes the maximum transfer ratio for transferable loads. $L_{IFL,t}$ denotes the reduction amount for interruptible load. δ_{IFL}^{max} denotes the maximum reduction amount for interruptible loads. L_t^0 denotes the total system load demand.

(6) Energy storage

The energy stored in a storage system is determined by the amount of energy stored at the previous time step and the charging or discharging amount at the current time step. Energy storage must adhere to constraints on charging and discharging power, state of charge, and energy balance. Energy storage costs primarily include charging costs, energy losses, and operation and maintenance costs; charging costs and energy losses are already accounted for in the model and do not need to be considered separately. The operational models for electrochemical storage and pumped storage are similar:

$$F_{ES,t} = \rho_{ES}^{dis} P_{ES,t}^{dis} \tag{24}$$

$$C_{ES,t} = C_{ES,t-1} + \eta_{ES} P_{ES,t}^{chr} - \frac{1}{\eta_{ES}} P_{ES,t}^{dis} \tag{25}$$

$$\mu_{ES,t}^{chr} P_{ES}^{chr,min} \leq P_{ES}^{chr} \leq \mu_{ES,t}^{chr} P_{ES}^{chr,max} \tag{26}$$

$$\mu_{ES,t}^{dis} P_{ES}^{dis,min} \leq P_{ES,t}^{dis} \leq \mu_{ES,t}^{dis} P_{ES}^{dis,max} \tag{27}$$

$$\mu_{ES,t}^{chr} + \mu_{ES,t}^{dis} \leq 1 \tag{28}$$

$$C_{ES}^{min} \leq C_{ES,t} \leq C_{ES}^{max} \tag{29}$$

$$C_{ES,1} = C_{ES,T} \tag{30}$$

where $F_{ES,t}$ denotes the operational cost of storage, ρ_{ES}^{dis} denotes the unit cost of storage per unit of electricity. $C_{ES,t}$ denotes the amount of energy stored. $P_{ES,t}^{chr}$ and $P_{ES,t}^{dis}$ denote the charging and discharging powers of the storage, respectively. η_{ES} denotes the charging and discharging efficiencies. $\mu_{ES,t}^{chr}$ and $\mu_{ES,t}^{dis}$ are 0-1 state variables for charging and discharging, respectively. $P_{ES}^{chr,min}$, $P_{ES}^{chr,max}$, $P_{ES}^{dis,min}$, $P_{ES}^{dis,max}$ denote the limits for charging and discharging power, respectively. C_{ES}^{min} and C_{ES}^{max} denote the maximum and minimum capacity limits of the storage, respectively. $C_{ES,1}$ and $C_{ES,T}$ denote the energy levels at the scheduling period's initial and final time steps, respectively. T denotes the scheduling period.

*Collaborative Operation Mechanism
for Flexible Resources*

Different flexibility resources of source, grid, load, and storage have distinct operational characteristics, with significant differences in adjustment ranges, ramp rates, and start-up speeds. The diversity of flexibility requirements in power systems is reflected in the timescale, requiring the accommodation of load fluctuations in the short term as well as resource optimization and allocation in the long term. In terms of regulation, flexibility requirements include upward regulation to address increased load and downward regulation to respond to load reductions. Regulation depth is characterized by varying degrees of resource adjustment capacity to accommodate different scales of supply and demand changes. The development of each flexibility resource has its associated strengths, weaknesses, opportunities, and threats [27]. The flexibility requirements of power systems exhibit diverse characteristics, including varying time scales, adjustment directions, and depths of adjustment. Therefore, each type of resource provides complementary advantages in delivering flexibility to the power system. It is essential to comprehensively consider these flexible resources' economic costs and technical features, define their development roles clearly, and strategically combine and leverage their strengths while mitigating their weaknesses to achieve collaborative development of various flexible resources.

Specifically, coal-fired power transformation involves large existing units and currently offers certain economic advantages. Hydropower has significant adjustment potential in regions with abundant water resources and requires a well-planned annual water allocation. Transmission lines enable cross-regional optimization of resources, provide accommodation space for the sending end, and enhance supply security for the receiving end. Demand-side flexible loads have low investment costs and fast response rates, making them suitable for quickly addressing extreme events. Energy storage can shift energy across different time periods, transferring surplus renewable energy to peak load periods. The collaborative operation mechanism of source, grid, load, and storage resources is illustrated in Fig. 1.

The Collaborative Scheduling Model for Flexible Resources

Previous studies have obtained the operational characteristics of flexible resources from generation, grid, load, and storage (source-grid-load-storage) into mathematical models, achieving a unified description of different resources at the mathematical level. Then, a collaborative scheduling model for flexible resources is established based on the fundamental principles and requirements of power system operation. For example, the supply-demand balance of energy can be obtained as a power balance constraint, and the supply capacity of energy can be obtained as a system reserve constraint. These constraints ensure that the scheduling solution remains within the feasible domain, with various resources from generation, grid, load, and storage working together to maintain balance. For instance, different power sources provide energy,
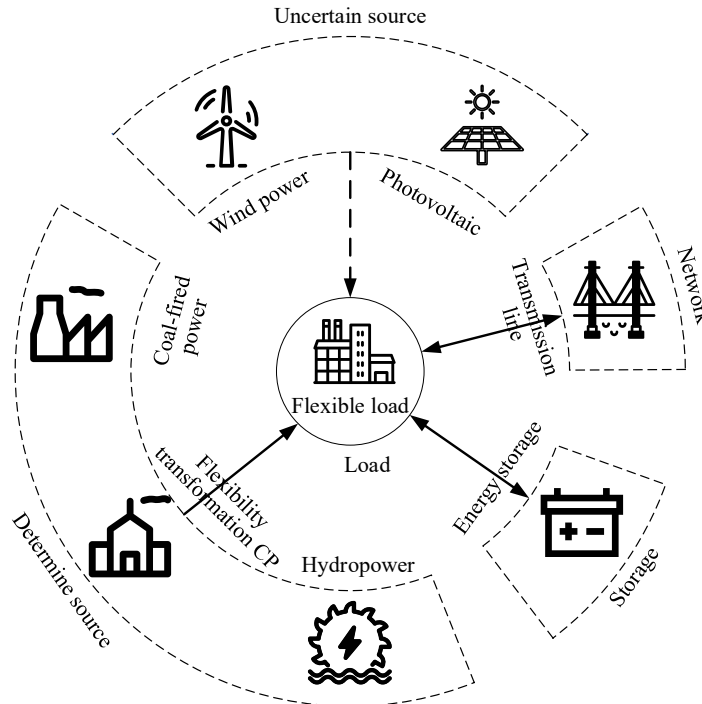

Fig. 1. Collaborative mechanism for flexibility resources.

loads represent the energy demand but can be flexibly adjusted, and storage can be seen as energy supply during discharging and energy demand during charging. The objective function of the collaborative scheduling model is to minimize the overall system operating cost. Optimization methods are used to perform global optimization under the premise of satisfying various constraints. In this process, the model considers the synergies between different resources until it finds the optimal combination of resources and scheduling strategy to achieve the best objective function.

Objective Function

When wind power and photovoltaic outputs are high, there is a risk of electricity supplies exceeding demand. When flexible resources have insufficient upward adjustment capability, wind power and photovoltaic curtailment may occur. Conversely, insufficient downward adjustment capability can lead to load-shedding events. Penalty terms are included in the objective function to prevent the curtailment of wind power, photovoltaics, and load shedding. The collaborative scheduling model integrates various types of flexible resources of source, grid, load, and storage into a unified optimization framework, with the objective function of minimizing comprehensive operation costs.

$$\min f = \sum_{i=1}^{I} \left(F_{CP,i,t}^{coal} + F_{CP,i,t}^{UD} \right) + \sum_{j=1}^{J} \left(F_{FTCP,j,t}^{coal} + F_{FTCP,j,t}^{UD} \right)$$
$$+ F_{HP,t} + F_{TL,t} + F_{FL,t} + F_{ES,t} + F_{RE,t} + F_{SL,t}$$

$$(31)$$

where $F_{RE,t}$ denotes the penalty cost for curtailment of wind power and photovoltaics, $F_{SL,t}$ denotes the penalty cost for load shedding. The calculations are as follows:

$$F_{RE,t} = \rho_{RE} \left(P_{WP,t}^{curt} + P_{PV,t}^{curt} \right)$$

$$(32)$$

$$F_{SL,t} = \rho_{SL} L_{SL,t}$$

$$(33)$$

where ρ_{RE} is the unit penalty cost for curtailment of wind power and photovoltaics, $P_{WP,t}^{curt}$ and $P_{PV,t}^{curt}$ denote the power of curtailment of wind power and photovoltaics, respectively. ρ_{SL} is the unit penalty cost for load shedding. $L_{SL,t}$ is the power associated with load shedding.

Constraints

In addition to the operational models for the various types of flexible resources mentioned above, the following constraints must be satisfied:

(1) Curtailment of wind power and photovoltaic constraints

When there is no curtailment of wind power and photovoltaics, the actual power output of wind power and photovoltaics is equal to the forecasted power output. When curtailment occurs, the actual power output of wind and photovoltaics is less than the forecasted power output.

$$P_{WT,t} = P_{WT,t}^0 - P_{WP,t}^{curt}$$

$$(34)$$

$$0 \le P_{WP,t}^{curt} \le P_{WT,t}^0$$

$$(35)$$

$$P_{PV,t} = P_{PV,t}^0 - P_{PV,t}^{curt}$$

$$(36)$$

$$0 \le P_{PV,t}^{curt} \le P_{PV,t}$$

$$(37)$$

where $P_{WT,t}$ and $P_{PV,t}$ denote the actual power of wind power and photovoltaics, respectively, $P_{WT,t}^0$ and $P_{PV,t}^0$ denote the forecasted power of wind power and photovoltaics, respectively.

(2) Power balance constraint

Power balance is a fundamental safety and stability issue in the power system. A traditional power system primarily focuses on balancing power generation and consumption at peak load times, which generally ensures balance at other times. However, the balancing standards are more complex in a new power system with a high proportion of renewable energy. Power consumption and generation need to be balanced in real time, relying on the adjustment capabilities of various flexible resources.

$$P_{WT,t} + P_{PV,t} + \sum_{i=1}^{I} P_{CP,i,t} + \sum_{j=1}^{J} P_{FTCP,j,t} + P_{HP,t} + \left(P_{ES,t}^{dis} - P_{ES,t}^{chr} \right)$$
$$= L_t^0 + P_{TL,t} + L_{TFL,t}^{in} - L_{TFL,t}^{out} - L_{IFL,t} - L_{SL,t}$$

$$(38)$$

(3) System reserve constraints

To ensure real-time power balance and to account for imbalances caused by renewable energy forecast deviations, load forecast errors, and various operational incidents, a certain amount of standby regulation capacity needs to be reserved. When deviations occur, the power supply-demand balance will be disrupted. At this point, the balance can be restored by adjusting the output. The auxiliary services mechanism includes various types, with reserves being the main focus of this study.

$$\sum_{i=1}^{I} \left(u_{i,t} \alpha_{CP,i}^{\max} C_{CP,i} - P_{CP,i,t} \right) + \sum_{j=1}^{J} \left(u_{j,t} \hat{\alpha}_{FTCP,j}^{\max} C_{FTCP,j} \right.$$
$$\left. - P_{FTCP,j,t} \right) \ge r_t^U L_t^0$$

$$(39)$$

$$\sum_{i=1}^{I}\left(P_{CP,i,t}-u_{i,t}\alpha_{CP,i}^{\min}C_{CP,i}\right)+\sum_{j=1}^{J}\left(P_{FTCP,j,t}\right.$$
$$\left.-u_{j,t}\hat{\alpha}_{FTCP,j}^{\min}C_{FTCP,j}\right)\leq r_t^D L_t^0 \qquad (40)$$

Where r_t^U and r_t^D denote the positive and negative reserve rates, respectively.

Robust Optimization Method Improvement

The above-mentioned collaborative scheduling model for flexible resources is deterministic. In traditional deterministic optimization scheduling models, the predicted power output of renewable energy is typically treated as the actual value. However, the reality is that predictions always have inevitable deviations. In practice, renewable energy generation is influenced by meteorological factors, such as wind speed, sunlight, and precipitation, resulting in uncertainty in output, which reduces the safety of system scheduling. Robust optimization theory can be employed to enhance decision robustness. The general form of a traditional robust optimization model is:

$$\begin{cases} \min \ \boldsymbol{c}^T\boldsymbol{x} \\ s.t. \ \ \boldsymbol{a}_i^T\boldsymbol{x}\leq\varpi_i^T\boldsymbol{b}_i, \ \ i=1,2,\cdots,n \end{cases} \qquad (41)$$

where $\boldsymbol{c}^T$ denotes the objective coefficients, $\boldsymbol{x}$ denotes the decision variables. $\boldsymbol{a}_i^T$ denotes the coefficients of the constraints. ϖ_i^T denotes the uncertain parameters. $\boldsymbol{b}_i$ denotes the uncertainty in the parameters.

The traditional robust optimization model requires that the above constraints be met under all circumstances, often leading to decisions based on the worst-case scenario, which rarely occurs in practice. This results in overly conservative decision-making. On the other hand, the number of hard constraints in the model is increased, making the model unsolvable. Therefore, traditional robust optimization models have some limitations.

This study makes some improvements to the traditional robust optimization model. Slack variables γ are introduced to relax the constraints in the traditional robust optimization model, allowing the model to violate some constraints within the uncertainty set range, meaning that the power of renewable energy can fluctuate within a certain interval. However, the violation of constraints is given a certain upper limit and converted into a loss cost included in the objective function. These adjustments are also in line with the actual operation of power systems. For example, when there is a power shortage, managers guide users to reduce electricity consumption through demand response and provide compensation, temporarily breaking the original supply-demand balance constraint by incurring some costs.

Therefore, relaxation variables γ are introduced to balance economic efficiency and security, transforming the robust optimization model into a light robust optimization model. Box-set constraints and 1-norm constraints are used to describe the polyhedral set of uncertain parameters [28].

$$\begin{cases} \min \ \boldsymbol{c}^T\boldsymbol{x}+\boldsymbol{d}^T\boldsymbol{\gamma} \\ s.t. \ \ \boldsymbol{a}_i^T\boldsymbol{x}-\gamma_i\leq\varpi_i^T\boldsymbol{b}_i, \ \ i=1,2,\cdots,I \\ \qquad 0\leq\gamma_i\leq\gamma_i^{\max}, \qquad i=1,2,\cdots,I \end{cases} \qquad (42)$$

$$\begin{cases} b_{i,j}=\overline{b}_{i,j}+\xi_{i,j}\hat{b}_{i,j} \quad j\in J_i, \xi_{i,j}\in\Omega \\ \Omega_i=\left\{\xi_{i,j} \ \middle| \ \left|\xi_{i,j}\right|\leq 1, \sum_j\left|\xi_{i,j}\right|\leq\Gamma_i\right\} \end{cases} \qquad (43)$$

where γ denotes the relaxation variables, $\boldsymbol{d}^T$ corresponds to the coefficient. $c_i^{\max}$ denotes the upper limit. $b_{i,j}$ denotes the j-th uncertain parameter in $\boldsymbol{b}_i$. $\overline{b}_{i,j}$ denotes the mean (predicted value) of the uncertain parameter $b_{i,j}$. $\hat{b}_{i,j}$ is the maximum fluctuation range. $\xi_{i,j}$ denotes the degree of fluctuation. Ω_i is the box uncertainty set for $\xi_{i,j}$. Γ_i controls the expected range of fluctuations, also called the robustness coefficient, and controls the total fluctuation amount.

This paper solves the light robust optimization model using an equivalent transformation approach. Equation (42) can be expressed as:

$$\boldsymbol{a}_i^T\boldsymbol{x}-\gamma_i\leq\sum_j\varpi_{i,j}^T\left(\overline{b}_{i,j}+\xi_{i,j}\hat{b}_{i,j}\right) \qquad (44)$$

Equation (44) equals:

$$\boldsymbol{a}_i^T\boldsymbol{x}-\gamma_i\leq\sum_j\varpi_{i,j}^T\overline{b}_{i,j}-\max\sum_j\left|\xi_{i,j}\right|\left|\varpi_{i,j}^T\hat{b}_{i,j}\right| \qquad (45)$$

To obtain the maximum value of $\left|\xi_{i,j}\right|\left|\varpi_{i,j}^T\hat{b}_{i,j}\right|$, we first sort $\left|\varpi_{i,j}^T\hat{b}_{i,j}\right|$ to get $\left|\varpi_{i,j}^T\hat{b}_{i,j}\right|'$. Since $\sum_j\left|\xi_{i,j}\right|\leq\Gamma_i$, the integer and fractional parts of Γ_i need to be truncated. Assume the floor of Γ_i is $\lfloor\Gamma_i\rfloor$. Then, the coefficients $\left|\xi_{i,j}\right|$ of the first $\lfloor\Gamma_i\rfloor$ terms of $\left|\varpi_{i,j}^T\hat{b}_{i,j}\right|'$ are assigned a value of 1 to ensure the maximum. The coefficient of the next term $\lfloor\Gamma_i\rfloor+1$ is assigned a value of $\Gamma_i-\lfloor\Gamma_i\rfloor$, and the remaining coefficients are set to zero. Thus, Equation (45) can be equivalently transformed into:

$$a_i^T x - \gamma_i \leq \sum_j \varpi_{i,j}^T \bar{b}_{i,j} - \sum_{j=1}^{\lfloor \Gamma_i \rfloor} \left| \varpi_{i,j}^T \hat{b}_{i,j} \right|' - \left(\Gamma_i \right.$$
$$\left. - \lfloor \Gamma_i \rfloor \right) \left| \varpi_{i,\lfloor \Gamma_i \rfloor+1}^T b_{i,\lfloor \Gamma_i \rfloor+1} \right|' \tag{46}$$

In the scheduling of source, grid, load, and storage flexibility resources, wind power, photovoltaic, and hydropower outputs all have certain uncertainties. However, wind power and photovoltaics have high uncertainties, while hydropower has relatively low uncertainty. Renewable energy generation is correlated, which is reflected in various aspects such as weather, geography, season, and time of day [29]. Multiple uncertainty factors may also have potential correlations. Therefore, there is a budget constraint on the total uncertainty. The corresponding uncertainty budget constraints can be expressed as:

$$\begin{cases} \left| \xi_{WT} \right| + \left| \xi_{PV} \right| + \left| \xi_{HP} \right| \leq \Gamma \leq 3 \\ \left| \xi_{WT} \right| \leq \Gamma_1 \leq 1 \\ \left| \xi_{PV} \right| \leq \Gamma_2 \leq 1 \\ \left| \xi_{HP} \right| \leq \Gamma_3 \leq 1 \end{cases} \tag{47}$$

where ξ_{WT}, ξ_{PV}, ξ_i denote the uncertain parameters for wind power, photovoltaic, and natural water inflow, respectively.

In summary, the scheduling model's Equation (38) is revised using the improved method's formula (46). Relaxation variables for curtailing wind power, solar power, and load shedding are introduced, allowing the power balance constraint to be relaxed at a certain operational cost, thereby characterizing the relationship between operational cost and management risk.

Curtailing wind power, solar power, and load shedding can also serve as indicators for assessing the operational risk of the power system. Additionally, the uncertainty budget coefficient can be used to limit the intensity of renewable energy output fluctuations, providing decision-making references for managers with different confidence levels and risk attitudes. The above model will be built in Matlab 2022, with the Gurobi solver used to find the optimal solution, resulting in the optimal collaborative combination of flexible resources.

Results and Discussion

Case Study Introduction

This paper uses a regional power system as an example for simulation. The region has abundant clean energy and is a power-exporting area. The maximum local load is 12.6 GW, and the maximum export load is 1.8 GW. The load curves for local and exported electricity are shown in Fig. 2. The proportion of transferable flexible loads is 3%, with a unit cost of 0.2 CNY/kWh, and the proportion of interruptible flexible loads is 2%, with a unit cost of 0.4 CNY/kWh. The load-shedding cost is 1 CNY/kWh. The reserve rates for both positive and negative reserves are 5%.

The installed capacity of coal-fired power is 12 GW, divided into six types comprising 26 units. The parameters of the coal-fired power units are shown in Table 2. After flexible transformation, one unit of each type can control the minimum power to 30%, improve the ramp-up rate to 50% of the rated power, and reduce the start-up and shut-down time. The installed capacity of hydropower is 0.3 GW, with a typical daily distributed generation of 1.6 GWh and a unit generation cost of 0.28 CNY/kWh. The installed capacity of energy storage is 1 GW, with a charge and discharge duration of
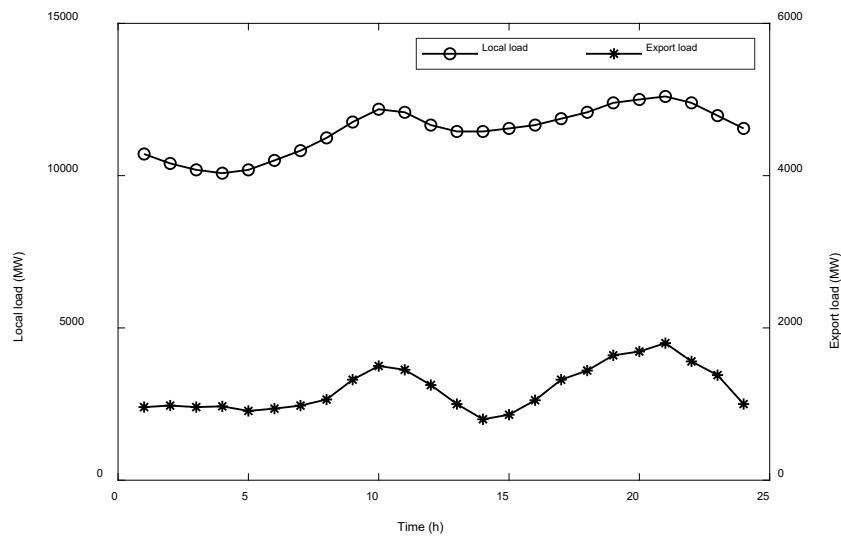

Fig. 2. The load curves for local and exported electricity.

Table 2. The parameters of the coal-fired power units.

No.	Quantity	Minimum power	Maximum power	Installed capacity (MW)	Ramp-up/Ramp-down (MW)	Coal consumption rate (t/MW)	Strat-up/shut down time (h)
1-3#	3	50%	100%	1000	0.3	0.2732	10
4-7#	4	50%	100%	600	0.3	0.2864	8
8-12#	5	50%	100%	550	0.3	0.2847	8
13-17#	5	50%	100%	400	0.3	0.2829	7
18-22#	5	50%	100%	250	0.3	0.2811	4
23-26#	4	50%	100%	150	0.3	0.2698	3

3 hours, a charge and discharge efficiency of 95%, and an operation and maintenance cost of 0.2 CNY/kWh. The installed capacity of wind power is 7.9 GW, and the installed capacity of photovoltaic power is 9.9 GW. The output of wind power and photovoltaics is predicted by considering their correlation. The forecasted wind power and photovoltaic power are shown in Fig. 3. The penalty cost for wind and solar curtailment is 0.2 CNY/kWh. Based on historical samples of wind power, photovoltaic power, and hydropower, the maximum fluctuation ranges are estimated to be 0.1 times, 0.08 times, and 0.05 times the forecast values, respectively, with an initial robustness factor of 2.4.

Case Study Results

The optimization model of the scenario in this paper considers flexible resources across all stages of the new power system, including source, grid, load, and storage. An improved robust optimization model is used to characterize the uncertainties of wind power, photovoltaic power, and hydropower. After solving the model, the operation costs of the power system are shown in Table 3. The operation costs are primarily due

to the fuel costs of coal-fired power, while the operation costs of other flexibility resources are relatively low. Additionally, there were no incidents of wind power and photovoltaic curtailment or load shedding. Under the collaborative adjustment mechanism of flexible resources (source, grid, load, and storage), the power system achieved full renewable energy consumption while ensuring system safety and stability.

On the power generation side, coal-fired power and hydropower adjust their output to track load and renewable energy fluctuations. The output power of coal-fired power and hydropower is shown in Fig. 4 and 5. At midday, coal-fired units reduce their output to make room for more photovoltaic generation. Additionally, six units were shut down, all of which had undergone flexibility retrofits. These retrofitted units feature faster ramp-up rates and shorter start-up and shut-down times, making them the preferred choice for deep peak shaving and start-stop regulation tasks. Compared to non-retrofitted units, those with flexibility upgrades exhibit stronger regulation capabilities. It can be observed that hydropower units have a fast regulation rate and can quickly increase output to their rated power at night, meeting the peak load demand. In contrast,
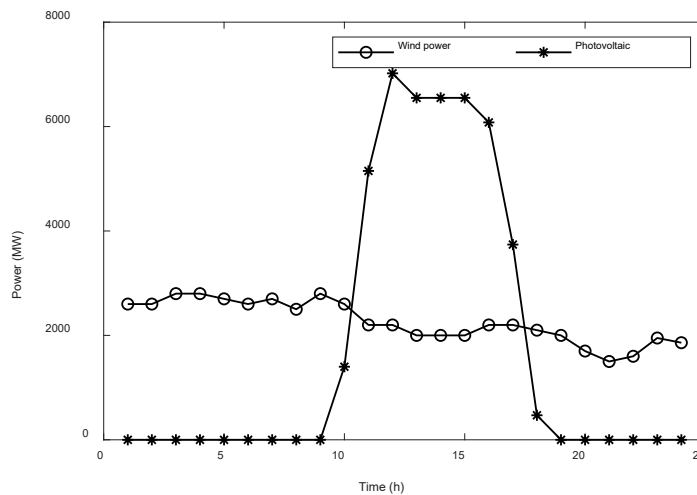

Fig. 3. The forecasted wind power and photovoltaic power.

Table 3. The operation costs of the power system (10^4CNY).

Item	Fuel	Up/down	Hydropower	Transmission line	Flexible load	Energy storage	Curtailment power	Load shedding	Total
Cost	4798	23.1	50.4	230.6	84.4	38.5	0	0	5225

coal-fired units have a relatively slower regulation rate, with their output power only able to gradually increase or decrease. In addition, the regulation range of hydropower is larger than that of coal-fired power units.

On the grid side, exporting high-proportion clean energy has promoted the region's integration of wind power and photovoltaics. The export load curve resembles the load curve of the receiving region, aligning with the load demand of the receiving region and ensuring a stable energy supply. A total of 28820 MWh of electricity was delivered. Transmission lines have optimized resource allocation across different spatial scales.

On the load side, flexible loads participate in demand response by adjusting their electricity usage time and amount. Fig. 6 shows the flexible load adjustments. The original power load curve has a "double peak and double valley" shape, particularly after the large photovoltaic generation at midday, where the net load (load minus wind and photovoltaic generation) exhibits a significant midday dip, creating pressure for photovoltaic absorption. At night, as photovoltaic generation sharply decreases, the net load shows a pronounced peak, generating higher electricity demand. To alleviate the typical intraday resource-time mismatch, flexible loads shift peak loads to low-demand periods and further reduce peak loads through load interruption. The total
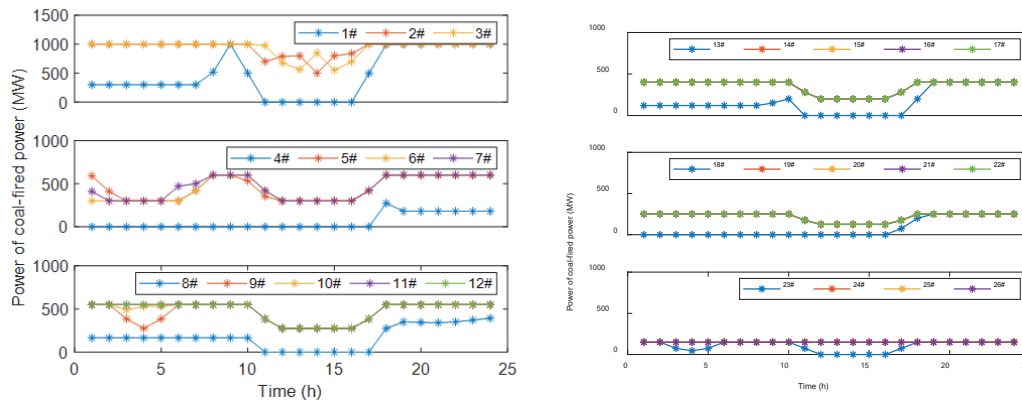

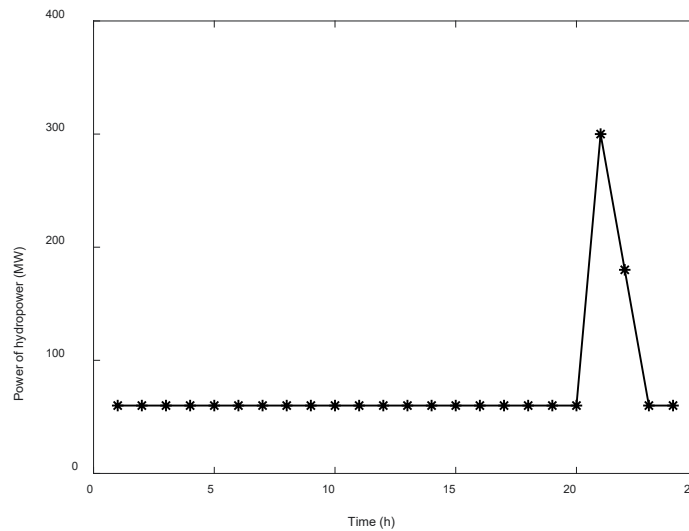Fig. 4. The output power of coal-fired power.
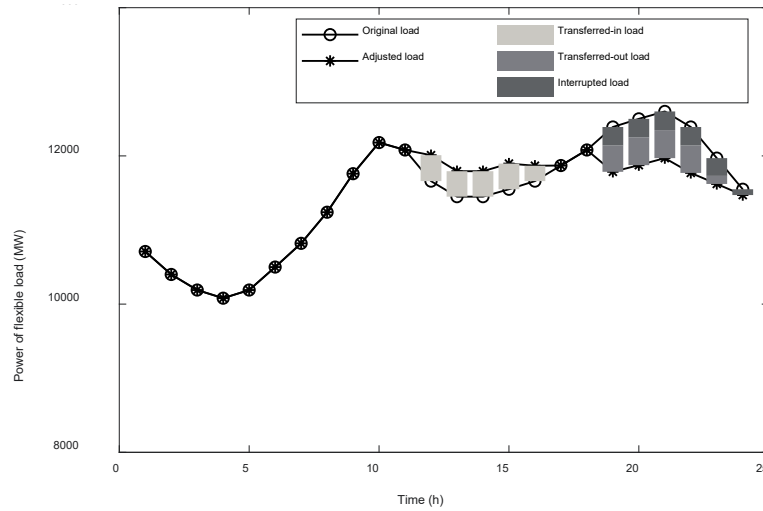

Fig. 5. The output power of hydropower.

Fig. 6. The flexible load adjustments.

flexible load transfer is 1590.5 MWh, and the total flexible load reduction is 1315.3 MWh.

After flexible load adjustments, the load curve becomes smoother, and the resource mismatch problem is somewhat alleviated on the demand side.

On the energy storage side, from Fig. 7, the energy, the energy storage system charges during the midday period of high photovoltaic generation, reaching its maximum charge at 15:00. The system discharges during the evening peak load period and then recharges to restore its initial state. The energy storage has a total charge of 2132.96 MWh and a discharge of 1952 MWh, with a utilization efficiency of 90%. The energy storage system plays a role in "peak shaving and valley filling," effectively transferring electricity across different time periods.

In summary, the various flexible resources of source, grid, load, and storage have different adjustment capabilities and patterns. A collaborative optimization and scheduling model can reasonably allocate these resources. The collaborative operation of these resources can track load trends, smooth out wind and photovoltaic fluctuations, and ensure real-time matching of power supply and demand.

Scenario Comparison

By setting different scenarios and comparing them with the scenario in this paper, the scenario settings are shown in Table 4. By comparing Scenario I and Scenario II with the scenario in this paper, the adaptability of the improved robust optimization model can be observed. The impact of different combinations of flexible resources on the power system is observed by comparing Scenario III to Scenario VI with the scenarios presented in this paper.

The operation costs of the power system under different scenarios are shown in Fig. 8. It can be observed that the cost of the traditional robust optimization model in Scenario I is higher than that of the improved robust optimization model in this paper's scenario. Although the traditional model provides greater security, its excessive conservativeness leads to some economic losses. In Scenario II, the deterministic optimization

Table 4. The scenario setting.

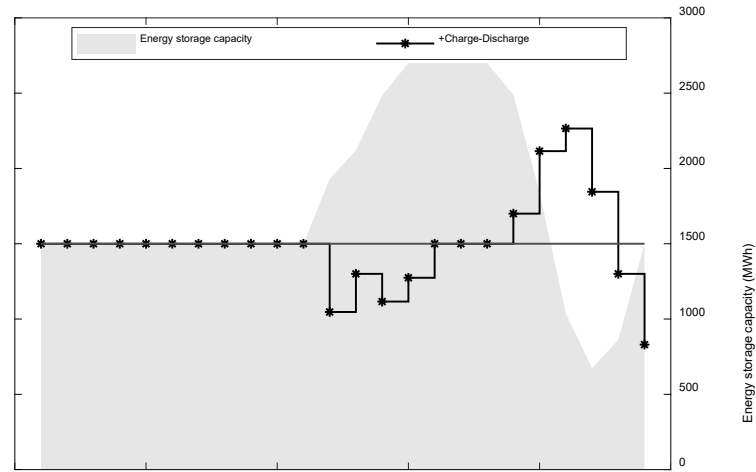| Scenario	Model			Flexibility resources			
	Certainty	Traditional Robust	Improved Robust	Flexible transformation coal-fired power	Transmission line	Flexible load	Energy storage
This Scenario			√	√	√	√	√
Scenario I		√		√	√	√	√
Scenario II	√			√	√	√	√
Scenario III			√		√	√	√
Scenario IV			√	√		√	√
Scenario V			√	√	√		√
Scenario VI			√	√	√	√	

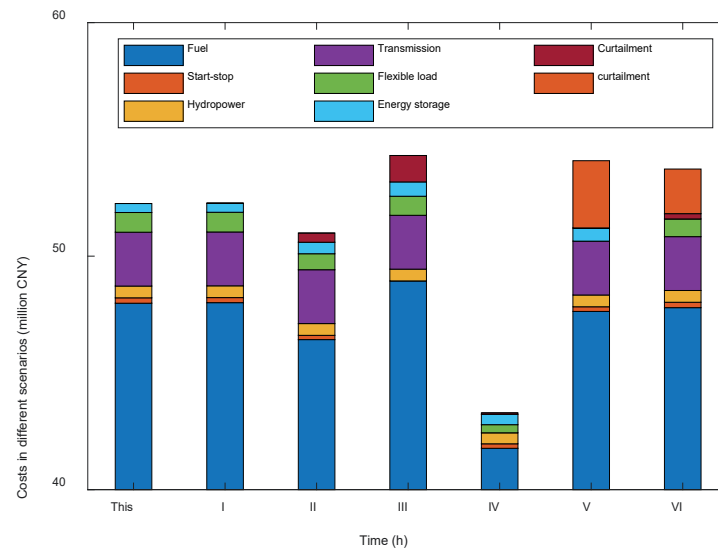Fig. 7. The charging and discharging power of energy storage.

Fig. 8. The cost structure under different scenarios.

model offers the best economic performance, but its scheduling plan lacks robustness, posing operational risks. The curtailment of wind and solar power was 1974.08 MWh. This indicator reveals that the deterministic optimization model carries a significant operational risk.

The operating cost of the improved robust optimization model in this study is lower than that of the traditional robust optimization model, avoiding the high costs associated with making extensive preparations for extremely low-probability scenarios, thus improving the conservatism of the decision-making process. Additionally, although the operating cost of the improved robust optimization model is higher than that of the deterministic optimization model in Scenario II, the curtailment of wind and solar power is 0, and this indicator is effectively controlled. The power system exhibits higher safety and reliability, which is the most fundamental prerequisite for the system's operation.

In summary, the improved robust optimization model strikes a balance between risk and cost, effectively reducing operational costs while ensuring system safety. Notably, the improved method also reduces difficulties in problem-solving. Decision-makers can control the operational strategy by setting the uncertainty budget coefficient and adjusting the power system's risk resilience to accommodate fluctuations in renewable energy output. The uncertainty budget coefficient enhances the model's flexibility and applicability, providing decision-making references for planners with different confidence levels and risk attitudes.

Coal-fired power serves as the backbone of the power system. In Scenario III, since the coal-fired units have not undergone flexibility transformation, they cannot be shut down to ensure power security and must continue operating at high minimum power levels, which crowds out wind power and photovoltaic generation. This results in significant wind power and photovoltaics curtailment
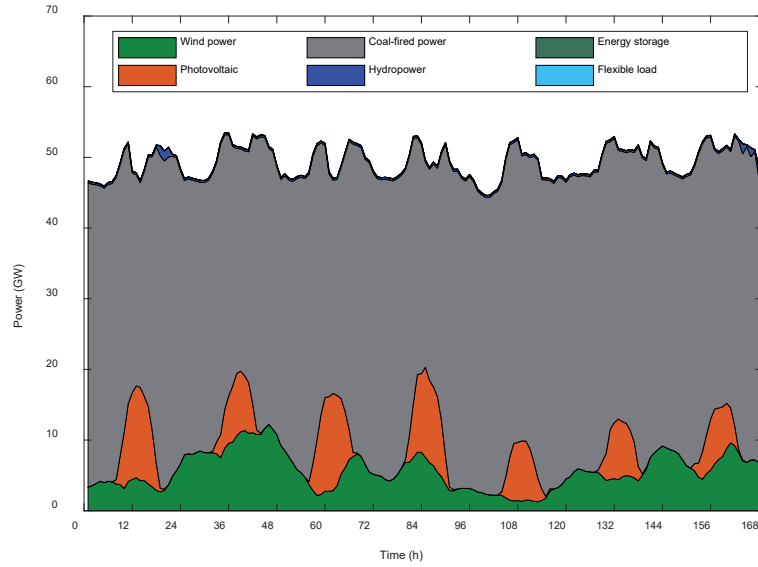
Fig. 9. Running simulation results of models in real scenes.

rates reaching as high as 6%. In Scenario IV, the absence of transmission lines prevents clean energy from being delivered to other regions, relying solely on local load consumption. However, the local consumption capacity is limited, leading to some wind power and photovoltaics curtailment. In Scenarios V and VI, the lack of flexible load and energy storage adjustment capabilities causes the power system to face load-shedding risks during the evening peak. At this time, photovoltaic generation is zero, wind power sharply decreases, and system load increases, making it impossible for coal-fired power alone to meet electricity demand.

The flexibility of the power system requires the joint contribution of flexible resources from all elements: source, grid, load, and storage. Every resource is indispensable for a power system with a high proportion of renewable energy. The core of power system operation is to ensure a real-time balance between power supply and demand. After subtracting the base load demand and the non-dispatchable volatile power sources (such as wind power and photovoltaics), the remaining gap must be filled by flexible resources. Different flexibility resources have different adjustment functions, and it is essential to scientifically combine various resources, leverage their strengths, avoid weaknesses, and coordinate their use to collectively meet the system's adjustment needs.

Discussion

This paper applies the aforementioned model to the power system in Western Inner Mongolia, extending existing research. On the one hand, the computational effectiveness of the model is discussed. On the other hand, the model's practicality and applicability are examined, and its performance in real-world scenarios and potential application limitations are observed.

The project takes the Western Inner Mongolia power system as a case study, selecting a typical week for simulation. The region has a relatively high renewable energy penetration rate compared to the rest of China. By the end of 2023, the installed capacity of wind and solar power reached 46.4%. The system includes nearly 200 coal-fired units and about 50 GW of wind and solar installed capacity. Detailed data can be found in reference [30]. When extending the model, additional variables, parameters, and constraint equations need to be added, with the principles remaining consistent with the current model. After the extension, the model was applied to a more complex power system, and the solution time was 12.29 seconds, which is still within an acceptable range, indicating that the computational difficulty of the model is manageable.

Fig. 9 shows the simulation results for the model in a real-world scenario. The results indicate that this study can improve the utilization of renewable energy, and no load-shedding events occurred during the typical week. The flexible resource collaborative optimization scheduling technology can achieve a reasonable distribution of electricity resources. The proposed improved robust optimization model balances both the economic and security aspects of power system operation. The model extension discussion reached conclusions consistent with the case study above, further validating the model's practicality and applicability.

Conclusions

This paper proposes an improved robust optimization scheduling model that coordinates multiple flexibility resources of source, grid, load, and storage to address the adjustment needs and operational risks brought by the high penetration of renewable energy in the new

power systems. A regional power system case study shows various flexible resources, such as flexible transformation coal-fired power, regulated hydropower, transmission lines, and flexible loads. Energy storage plays an irreplaceable role in the new power system. These resources effectively track load changes and mitigate wind power and photovoltaic fluctuations through collaborative optimization and scheduling. Collaborative scheduling achieves complementary advantages and optimal allocation among different resources, which is crucial for the stable operation of a power system with high renewable energy penetration. The improved robust optimization model ensures full absorption of renewable energy while reducing system operation costs, balancing risk and economy better than traditional robust optimization and deterministic optimization models. To enhance the flexibility of power systems with a high proportion of renewable energy, it is necessary to adopt diversified strategies and design corresponding incentive mechanisms to encourage the active participation of flexibility resources in system regulation. Specific measures include accelerating the flexible transformation of coal-fired power plants, expanding the scale of energy storage facility deployment, and tapping into the potential of demand-side flexible load regulation.

As wind power and photovoltaic capacities increase, the amplitude of power fluctuations becomes more pronounced, and hour-level optimization models are insufficient to reflect the actual operation of the power system. Future research will extend to multiple time scales, including more detailed short-time scales (such as minute-level) and the coordination between different time scales. This will require the model to have dynamic rolling and real-time updating capabilities, which may need to be addressed using Model Predictive Control (MPC) theory. Over time, the scheduling approach should be continuously updated based on the real-time changes in renewable energy generation and demand. Additionally, the model's understanding of uncertain information is still insufficient, as it currently only considers forecast errors without accounting for other practical scenarios. The uncertainty of load will also impact the power system. Future work will focus on incorporating more uncertainty factors.

Acknowledgments

Conflict of Interest

The authors declare no conflict of interest.

References

1. ZHANG D., ZHU Z., CHEN S., ZHANG C., LU X., ZHANG X., ZHANG X., DAVIDSON M.R. Spatially resolved land and grid model of carbon neutrality in China. Proceedings of the National Academy of Sciences, **121** (10), e2306517121, **2024**.

2. WANG Y., WANG R., TANAKA K., CIAIS P., PENUELAS J., BALKANSKI Y., SARDANS J., HAUGLUSTAINE D., LIU W., XING X., LI J., XU S., XIONG Y., YANG R., CAO J., CHEN J., WANG L., TANG X., ZHANG R. Accelerating the energy transition towards photovoltaic and wind in China. Nature, **619** (7971), 761, **2023**.

3. FANG X., CUI H., YUAN H., TAN J., JIANG T. Distributionally-robust chance constrained and interval optimization for integrated electricity and natural gas systems optimal power flow with wind uncertainties. Applied Energy, **252**, 113420, **2019**.

4. JIANG Z., HAN J., LI Y., CHEN X., PENG T., XIONG J., et al. Charging station layout planning for electric vehicles based on power system flexibility requirements. Energy, **283**, 128983, **2023**.

5. LIANG Y., KLEIJN R., VAN DER VOET E. Increase in demand for critical materials under IEA Net-Zero emission by 2050 scenario. Applied Energy, **346**, 121400, **2023**.

6. HUANG M., CHANG J., GUO A., ZHAO M., YE X., LEI K., PENG Z., WANG Y. Cascade hydropower stations optimal dispatch considering flexible margin in renewable energy power system. Energy, **285**, 129375, **2023**.

7. WANG C., SONG J. Performance assessment of the novel coal-fired combined heat and power plant integrating with flexibility renovations. Energy, **263**, 125886, **2023**.

8. JIN X., LIU B., LIAO S., CHENG C., ZHANG Y., JIA Z. Assessing hydropower capability for accommodating variable renewable energy considering peak shaving of multiple power grids. Energy, **305**, 132283, **2024**.

9. QIN B., WANG H., LIAO Y., LI H., DING T., WANG Z., LI F., LIU D. Challenges and opportunities for long-distance renewable energy transmission in China. Sustainable Energy Technologies and Assessments, **69**, 103925, **2024**.

10. CUI J., RAN Z., SHEN W., XIN Y. Study on multi-type flexible load control method of active distribution network based on dynamic time-sharing electricity price. Applied Energy, **357**, 122479, **2024**.

11. CHEN X., WANG Y., WU Z., ZHOU M., YUAN B. Capacity expansion model for multi-temporal energy storage in renewable energy base considering various transmission utilization rates. Journal of Energy Storage, **98**, 113145, **2024**.

12. WANG J., ZENG P., YIN L., DONG Y., LIU X., YANG R. A two-stage distributed stochastic planning method for source-grid-load-storage flexibility resources considering flexible ramp capacity. International Journal of Electrical Power & Energy Systems, **160**, 110134, **2024**.

13. HAO J., FENG X., CHEN X., JIN X., WANG X., HAO T., HONG F., DU X. Optimal scheduling of active distribution network considering symmetric heat and power source-load spatial-temporal characteristics. Applied Energy, **373**, 123974, **2024**.

14. YANG L., JIANG Y., CHONG Z. Optimal scheduling of electro-thermal system considering refined demand response and source-load-storage cooperative hydrogen production. Renewable Energy, **215**, 118845, **2023**.

15. XIANG S., XU D., WANG P., BAI Z., ZENG L. Optimal expansion planning of 5G and distribution systems considering source-network-load-storage coordination. Applied Energy, **366**, 123372, **2024**.

16. KUNYA A.B., ABUBSKAR A.S., YUSUF S.S. Review of economic dispatch in multi-area power system: State-of-the-art and future prospective. Electric Power Systems Research, **217**, 109089, **2023**.

17. LI Y., YUAN J., CHEN S., WU Y. Optimal wind power capacity decision consider commitment contracts under uncertain power supply and electricity demand in China. Renewable and Sustainable Energy Reviews, **201**, 114629, **2024**.

18. FAN W., TAN Z., LI F., ZHANG A., JU L., WANG Y., DE G. A two-stage optimal scheduling model of integrated energy system based on CVaR theory implementing integrated demand response. Energy, **263**, 125783, **2023**.

19. XIAO M, ZHOU Q, ZHANG Z, YIN J. Real-Time Intrusion Detection in Power Grids Using Deep Learning: Ensuring DPU Data Security. HighTech and Innovation Journal, **5** (3), 814, **2024**.

20. KIM S., CHOI D.G. A sample robust optimal bidding model for a virtual power plant. European Journal of Operational Research, **316** (3)**,** 1101, **2024**.

21. ATTARHA A., AMJADY N., CONEJO A.J. Adaptive robust AC optimal power flow considering load and wind power uncertainties. International Journal of Electrical Power & Energy Systems, **96**, 132, **2018**.

22. ESTEBAN-PEREZ A., MORALES J.M. Distributionally robust optimal power flow with contextual information. European Journal of Operational Research, **306** (3), 1047, **2023**.

23. ZHAI J., JIANG Y., LI J., JONES C.N., ZHANG X. Distributed adjustable robust optimal power-gas flow considering wind power uncertainty. International Journal of Electrical Power & Energy Systems, **139**, 107963, **2022**.

24. ESFAHANI M., ALIZADEH A., AMJADY N., KAMWA I. A distributed VPP-integrated co-optimization framework for energy scheduling, frequency regulation, and voltage support using data-driven distributionally robust optimization with Wasserstein metric. Applied Energy, **361**, 122883, **2024**.

25. LEI C., WANG Q., ZHOU G., BU S., ZHOU N., LIN T., WEI F. Probabilistic wind power expansion planning of bundled wind-thermal generation system with retrofitted coal-fired plants using load transfer optimization. International Journal of Electrical Power & Energy Systems, **151**, 109145, **2023**.

26. RANABOLDO M., ARAGUES-PENALBA M., ARICA E., BADE A., BULLICH-MASSAGUE E., BURGIO A., CACCAMO C., CAPRARA A., CIMMINO D., DEMONCECH B., DONOSO I., FRAGAPANE G., GONZALEZ-FONT-DE-RUBINAT P., JAHNKE E., JUANPERA M., MANAFI E., ROVEKAMP J., TANI R. A comprehensive overview of industrial demand response status in Europe. Renewable and Sustainable Energy Reviews, **203**, 114797, **2024**.

27. CRUZ-PÉREZ N, RODRÍGUEZ-ALCÁNTARA J.S, KORONAIOU V.L.P., JANČULA A., RODRÍGUEZ-MARTÍN J., GARCÍA-GIL A., FONTES J.C., SANTAMARTA J.C. SWOT Analysis of the Benefits of Hydropower Energy in Four Archipelagos. Civil Engineering Journal, **10** (7), 2370, **2024**.

28. SILVA-RODRIGUEZ L., SANJAB A., FUMAGALLI E., VIRAG A., GIBESCU M. A light robust optimization approach for uncertainty-based day-ahead electricity markets. Electric Power Systems Research, **212**, 108281, **2022**.

29. SHAME B.H., TJAHJANA D.D.D.P., AZIZ M., MBUMBA M.T. Analysis of Seasonal Wind Energy Potential on Zanzibar Coastal Island. HighTech and Innovation Journal, **5** (2), 331, **2024**.

30. LIU G., DOU D., WANG Y., LI X., GAO Z., LV H. Multi-scenario flexibility requirement analysis of high proportion of new energy access to power system. Clean Energy, **8** (6), 187, **2024**.